AJNR

A New Method for Analyzing Histograms of Brain Magnetization Transfer Ratios: Comparison with Existing Techniques

Liang Qiang Zhou, Yue Min Zhu, Jérôme Grimaud, Marc Hermier, Marco Rovaris and Massimo Filippi

AJNR Am J Neuroradiol 2004, 25 (7) 1234-1241
http://www.ajnr.org/content/25/7/1234

A New Method for Analyzing Histograms of Brain Magnetization Transfer Ratios: Comparison with Existing Techniques

Liang Qiang Zhou, Yue Min Zhu, Jérôme Grimaud, Marc Hermier, Marco Rovaris, and Massimo Filippi

BACKGROUND AND PURPOSE: **Previously reported quantitative parameters for the magnetization transfer ratio (MTR) do not give identical results, which can limit their ability to differentiate normal from diseased tissue and render them vulnerable to variations among MR systems. Our purpose was to systematically study different MTR metrics; propose a new MTR histogram parameter, $AMTR_{2/3}$; and compare $AMTR_{2/3}$ with existing parameters in a study of multiple sclerosis (MS).**

METHODS: **Seven conventional MTR parameters were proposed: global and mean MTR; peak height and position of the histogram; and percentiles MTR_{25}, MTR_{50}, and MTR_{75}. Additionally, we investigated a parameter, $AMTR_{2/3}$, to indicate the normalized pixel count (area under the histogram curve) inside the band size of two-thirds MTR histogram peak height. All parameters were measured in 10 patients with relapsing-remitting MS (group A), 10 healthy control subjects from the same imaging center as that of patients (group B), and four healthy control subjects from an outside institution (group C). Comparison of findings was performed between groups A and B to assess the discriminating ability of MTR parameters and groups B and C to evaluate intersystem variations.**

RESULTS: **All MTR parameters differed between groups A and B, but the difference was significant for only global MTR, mean MTR, MTR_{25}, and $AMTR_{2/3}$. With the exception of $AMTR_{2/3}$, all parameters differed significantly between the two control groups.**

CONCLUSION: **$AMTR_{2/3}$ is less sensitive to MR imaging system variations than are other MTR parameters and was most effective in differentiating patients with MS from healthy control subjects. This finding supports the use of $AMTR_{2/3}$ in multicenter MT MR imaging studies of MS.**

Magnetization transfer (MT) imaging is now a well-recognized MR imaging technique for studying various brain diseases. For example, in its application to the study of multiple sclerosis (MS), MT MR imaging provides quantitative information about microscopic and macroscopic lesion burden, with some specificity for the most destructive aspects of MS (1, 2).

The first step in the quantitative analysis of MT MR imaging data is the calculation of the MT ratio (MTR). When this technique was initially developed, MTR values were obtained from regions of interest, which allowed the study of individual lesions and of discrete areas of brain tissue (3). Currently, MTR values are calculated on a pixel-by-pixel (or voxel-by-voxel) basis from a large area of brain tissue or from the entire brain parenchyma (4). With the current method, the histogram of MTR values is calculated for a more objective, global, and automated analysis of brain tissue.

To perform quantitative MTR histogram analysis, we applied several histogram parameters that have been proposed in the literature. Figure 1 shows the most frequently used parameters. These include the peak height and peak position of the histogram; the mean MTR; and the MTR values corresponding

Received April 9, 2003; accepted after revisions February 18, 2004.

From CREATIS, CNRS UMR 5515 and INSERM 4630 (L.Q.Z., Y.M.Z., J.G., M.H.), Hospital of Neurology of Lyon (M.H.), and Hospital Louis Pasteur (J.G.), Chartres, France, Neuroimaging Research Unit, Department of Neurology, Scientific Institute and University H San Raffaele, Milan, Italy (M.R., M.F.).

L.Q.Z. supported by the French Ministry, Ministere de l'Education Nationale, de la Recherche et de la Technologie, with grant Bourse post doctorant etranger. This work also partially support by the Region Rhone-Alpes under grant Ademo. J.G. supported by grants from the Hospices Civil de Lyon and the Centre National de la Recherche Scientifique.

Address reprint requests to Y.M. Zhu, CREATIS, Bat. B. Pascal, INSA Lyon, 69621 Villeurbanne Cedex, France.

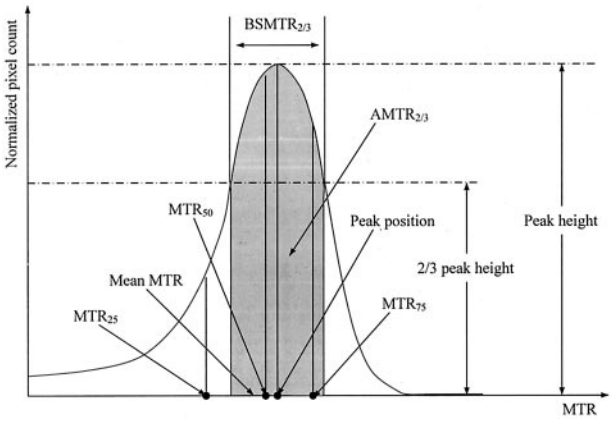

FIG 1. Graphical representation of the MTR histogram–derived parameters used in this study.

to the 25th (MTR_{25}), 50th (MTR_{50}), and the 75th (MTR_{75}) percentiles of the histogram, which indicate the MTR at which the integral of the histogram is 25%, 50%, and 75% of the total, respectively. All of these MTR metrics can be used to differentiate patients with MS from healthy control subjects (4, 5). They are correlated with the clinical manifestations of MS (5, 6) and are sensitive to the accumulation of disease burden over time (7). However, values obtained from established MTR parameters vary, and debate persists regarding which is the optimal histogram-derived parameter for large-scale, multicenter MS studies that require a tradeoff between sensitivity to disease-related changes and intersystem variability in measurements (4, 5, 8). The purpose of our study was to systematically investigate MTR histogram metrics and to propose a new histogram parameter, $AMTR_{2/3}$.

Methods

Participants

We examined 10 patients (group A, six women and four men) with relapsing-remitting MS (9). Mean age ± SD was 38.5 ± 9.2 years, mean duration of disease was 6.5 years (range, 1–15 years), and mean Expanded Disability Status Scale score (10) was 2.2 (range, 1.5–4.0). No patient had relapses or steroid treatment in the 3 months preceding study initiation. Ten healthy volunteers from the same imaging center (group B, seven women, three men) served as control subjects. Mean age was 33.5 ± 3.6 years. All subjects provided written informed consent.

To assess changes in the MTR histogram due to variation among MR imaging units, we examined four healthy control subjects (group C, one woman and three men). These subjects underwent MR imaging at another imaging center. Their mean age was 29.3 ± 8.2 years.

In groups A and B, cranial MR images were obtained by using a 1.5-T MR imaging unit (Magnetom Vision; Siemens Medical Systems, Erlangen, Germany). During a single imaging session, the following sequences were performed without moving the subject from the imager: 1) dual-echo turbo spin-echo (TSE) (TR/TE/NEX, 3300/16–98/1; echo train length, 5); 2) T1-weighted conventional spin-echo (TR/TE/NEX, 768/15/2); and 3) 2D gradient-echo (GE) (TR/TE, 640/12; flip angle, 20°) first with and then without an MT saturation pulse. (The latter was an off-resonance radio-frequency pulse centered 1.5 kHz below the water frequency with a Gaussian envelope of duration of 7.68 ms and a flip angle of 500°.) Twenty-four contiguous axial sections were acquired with a 5-mm section thickness, a 256 × 256 matrix, and a 250-mm field of view, giving an in-plane spatial resolution of approximately 1 × 1 mm. The sections were positioned parallel to a line joining the most inferoanterior and inferoposterior parts of the corpus callosum (11).

Subjects in group C underwent 2D GE imaging with the same type of 1.5-T MR imaging unit (Magnetom Vision) and parameters (TR/TE, 650/15; flip angle, 20°; first with and then without MT saturation pulse [off-resonance resonance radio-frequency pulse centered 1.5 kHz below the water frequency; Gaussian envelope of duration, 7.68 ms; and flip angle, 500°]) as those used in the other control group. Thirty-two contiguous axial sections were acquired with a 3-mm section thickness, a 256 × 256 matrix, and a 250-mm field of view, giving an in-plane spatial resolution of approximately 1 × 1 mm. The sections were positioned parallel to a line joining the most inferoanterior and inferoposterior parts of the corpus callosum.

Image Postprocessing

For each subject, only 10 central sections (groups A and B) or 18 central sections (group C) were postprocessed; these represented an axial slab of brain tissue with 5- or 5.4-cm thickness, respectively. This brain volume was chosen to minimize the inclusion of extracerebral tissue in the histogram (4). Two GE images, one with and one without a saturation pulse, and two TSE images (groups A and B) obtained at the same position as that of corresponding GE images were first registered. Then, an automatic segmentation algorithm based on a k-Nearest-Neighborhood (k-NN) clustering method was applied to the TSE images (group A and B) or to the GE images (group C) to remove hypointense pixels, such as those for background noise and bone. An image-processing technique of mathematical morphology was finally performed to remove extra cerebral tissues. After postprocessing, only brain tissue (ie, white matter, gray matter, CSF, and MS lesions) was kept, and a template of each brain was created.

MTR Histogram Analysis

An MTR map corresponding to each section was created. All pixels with MTR values lower than 10% were excluded to minimize the number of residual pixels with partial volume averaging from CSF (12). To correct for the between-subject difference in brain volume, each histogram was normalized by dividing it by the total number of pixels in the brain volume under consideration. From each normalized MTR histogram, band size of two-thirds histogram peak height ($BSMTR_{2/3}$) and the area under the histogram curve ($AMTR_{2/3}$) were calculated. For comparison, the following MTR histogram measures were calculated: mean brain MTR, peak height, peak position, MTR_{25}, MTR_{50}, and MTR_{75}. Global MTR of the brain parenchyma, which is not derived from MTR histograms, was also calculated. Global MTR was obtained by computing the mean signal intensity of the images obtained with and those without a saturation pulse corresponding to the total brain volume and then applying the MTR equation (3, 12).

MTR histograms obtained in patients with MS and healthy control subjects were visually compared. The discriminating ability of the MTR parameters was studied in terms of the mean, SD, SD/mean ratio, relative difference, and results of a two-tailed Student t test for unpaired data. Statistical significance was set at $P < .001$. Differences in the patient and control groups were also visually assessed by expressing an MTR histogram parameter as a function of the number of subjects.

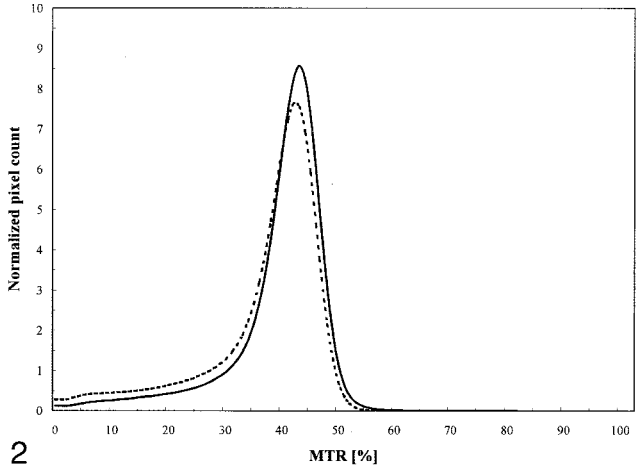

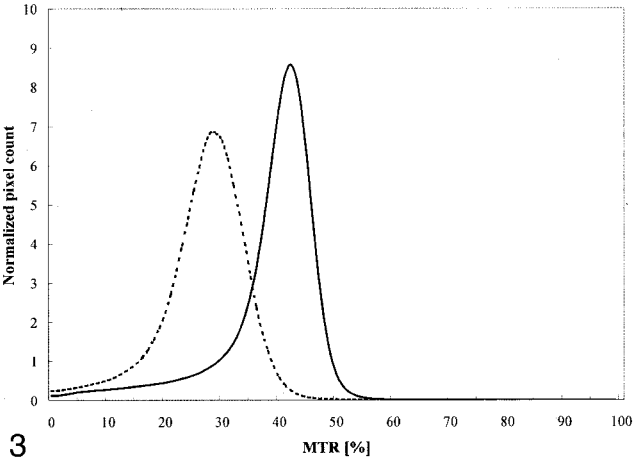

FIG 2. Average MTR histograms from 10 patients with MS (*dotted line*) and 10 healthy control subjects (*solid line*) obtained by using the same MR imaging unit.

FIG 3. Average MTR histograms from groups B (*solid line*) and C (*dotted line*), the two control groups, who were imaged with different MR imaging units.

TABLE 1: MT MR imaging–derived parameters in subjects imaged with the same imaging system

Parameter	MS Patient Group A (n = 10)		Healthy Control Group B (n = 10)		Relative Difference	P Value
	Mean ± SD	SD/Mean	Mean ± SD	SD/Mean		
Global MTR	37.19 ± 1.44	3.87%	38.97 ± 1.07	2.75%	−4.69%	.006
Mean MTR	37.37 ± 1.43	3.83%	39.11 ± 1.04	2.65%	−4.55%	.006
MTR histogram peak height	8.28 ± 0.55	6.64%	8.99 ± 1.03	11.45%	−8.14%	.07
MTR histogram peak position	41.30 ± 1.34	3.24%	42.10 ± 0.88	2.09%	−1.92%	.10
MTR_{25}	34.70 ± 1.64	4.73%	36.90 ± 1.29	3.49%	−6.15%	.004
MTR_{50}	39.60 ± 1.35	3.41%	40.70 ± 1.06	2.60%	−2.74%	.06
MTR_{75}	42.60 ± 1.35	3.17%	43.60 ± 0.97	2.22%	−2.32%	.07
$AMTR_{2/3}$	52.23 ± 1.46	2.80%	57.03 ± 2.47	4.33%	−8.79%	<.001
$BSMTR_{2/3}$	6.94 ± 0.53	7.64%	6.77 ± 0.86	12.70%	+2.40%	.60

Results

MTR histograms from patients with MS (group A) and same-center healthy control subjects (group B) had different shapes (Fig 2). The most salient changes in the patient group compared with those in the control group were a simultaneous decrease in histogram peak height and an increase in pixel counts at lower MTR values. These changes are quantitatively shown in Table 1, which also gives the quantitative assessment of the ability of each parameter to differentiate patients with MS from healthy control subjects. All MTR measurements differed between groups A and B. Moreover, all measurements except for $BSMTR_{2/3}$ had lower values in group A as compared with group B. However, the MTR parameters did not yield identical results. In particular, group differences were statistically significant for only global MTR (P = .006), mean MTR (P = .006), MTR_{25} (P = .004), and $AMTR_{2/3}$ (P <.001).

Difference in shape was also observed between MTR histograms from the two control groups, B and C, that underscore variations in findings due to different MR imaging systems (Fig 3). In particular, a marked shift and an important modification in lower MTR values on the histogram were observed between groups B and C. Table 2 shows the results of further assessment of their differences observed with different MTR parameters. A significant difference between the two control groups was found for all parameters, with the exception of $AMTR_{2/3}$.

Distinction between the patients (group A) and the same-center control subjects (group B) based on peak height, MTR_{25}, and $AMTR_{2/3}$ is graphically illustrated in Figures 4–6. Two MTR parameter curves were plotted to represent the patient (group A) and control (group B) participants. For each pair of parameter curves, an optimal MTR parameter value provided the best separation of the two groups. These values were 8.9, 36.1, and 54.7 for peak height, MTR_{25}, and $AMTR_{2/3}$, respectively.

Discussion

Fundamental Theoretical Basis of MT Imaging

The most primary information obtained from MT imaging is the MTR map that is obtained by calculating, on a pixel-by-pixel or voxel-by-voxel basis, the contrast between two images or two volumes acquired

TABLE 2: MT MR imaging–derived parameters in control subjects imaged with different imaging systems

Parameter	Control Group B (n = 10)		Control Group C (n = 4)		Relative Difference	P Value
	Mean ± SD	SD/Mean	Mean ± SD	SD/Mean		
Global MTR	38.97 ± 1.07	2.75%	27.56 ± 0.97	3.53%	34.31%	<.001
Mean MTR	39.11 ± 1.04	2.65%	27.69 ± 0.96	3.45%	34.19%	<.001
MTR histogram peak height	8.99 ± 1.03	11.45%	7.23 ± 0.52	7.17%	21.73%	.007
MTR histogram peak position	42.10 ± 0.88	2.09%	28.75 ± 0.96	3.34%	37.69%	<.001
MTR_{25}	36.90 ± 1.29	3.49%	24.00 ± 1.41	5.89%	42.36%	<.001
MTR_{50}	40.70 ± 1.06	2.60%	28.00 ± 0.82	2.92%	36.97%	<.001
MTR_{75}	43.60 ± 0.97	2.22%	31.75 ± 0.96	3.02%	31.45%	<.001
$AMTR_{2/3}$	57.03 ± 2.47	4.33%	59.50 ± 1.55	2.62%	4.25%	.091
$BSMTR_{2/3}$	6.77 ± 0.86	12.70%	9.25 ± 0.57	6.16%	30.92%	<.001

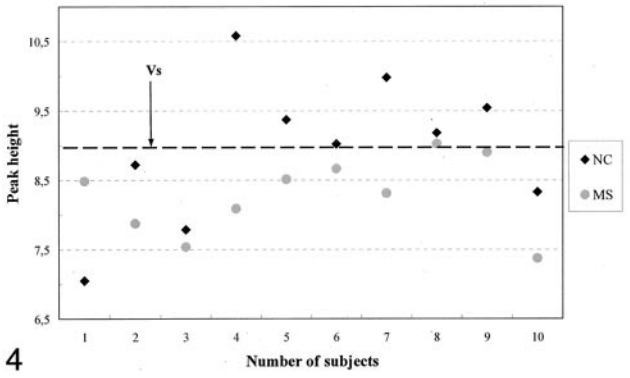

4

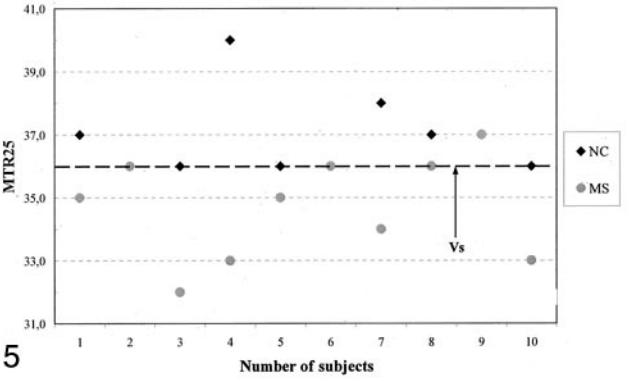

5

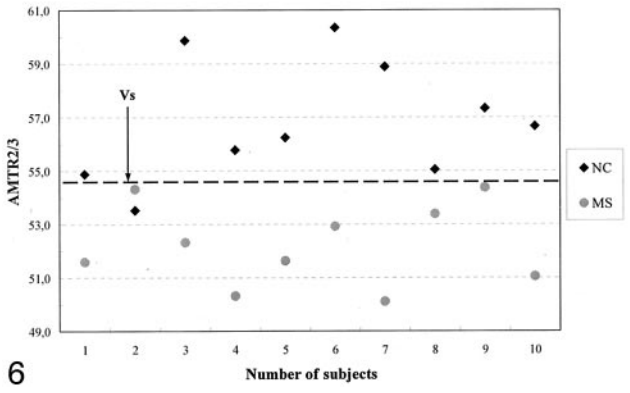

6

FIG 4. Scatterplot of MTR histogram peak heights indicates the value that best distinguished patients with MS and the control group B.

FIG 5. Scatterplot of MTR_{25} values indicates the value that best distinguished patients from the control group B.

FIG 6. Scatterplot of $AMTR_{2/3}$ values indicates that $AMTR_{2/3}$ was the best parameter for differentiating patients from control subjects.

first with and then without MT saturation. MT imaging of disease then consists of characterizing changes on the MTR map. If the MTR map is considered to be a simple 2D image or 3D volume, then many opportunities exist for exploiting such a 2D or 3D representation. Until this study, the most-explored parameter has been the histogram of the MTR map, which is measured by first counting the number of each MTR value (ie, the pixel count) and then dividing the pixel count by the total number of pixels or voxels included in the brain section or volume under consideration.

The mathematical nature of histogram analysis is the first-order probability density distribution, because a histogram is an approximation of the continuous probability density distribution in the cases of discrete images. Therefore, an implicit hypothesis of MTR histogram analysis is that the MTR map can be completely characterized by its probability density distribution. Under this assumption, MT imaging is reduced to a description of MTR histograms derived by quantitative parameters.

As shown in Figure 1, the previously proposed parameters exploit the histogram of the MTR map in a one-dimensional manner, since they all depend on one variable. The peak height parameter depends on only one MTR value. From a theoretical viewpoint, this parameter should not be used, as taking a single value of probability density distribution is illogical. Because MTR maps are discrete images, in practice we are not using a continuous probability density distribution but rather its discrete approximation; therefore, the peak height parameter can still be used. However, such a parameter is sensitive to spurious factors such as noise. The peak position and mean MTR are also of one dimension, because they depend on a single MTR value. The peak height, peak position, and mean MTR essentially describe changes of

the MTR histogram at a punctual position of the horizontal axis. They can only indirectly reflect changes in pixel counts besides those of the histogram peak or mean MTR value, and they do not give any indication of changes in pixel counts at lower MTR values. Therefore, they cannot allow one to completely describe changes in MTR histograms. MTR_{25}, MTR_{50}, and MTR_{75} are a class of parameters differing from the aforementioned peak height, peak position, and mean MTR parameters, because they involve integration of the MTR histogram over an interval or band of MTR values. However, since this integration is conditioned by the area percentage, the value of MTR_{25}, MTR_{50}, and MTR_{75} depends on only the upper limit of the interval (the lower limit of the interval is always fixed at zero). Therefore, the MTR_{25}, MTR_{50}, and MTR_{75} remain at one dimension. These parameters describe only changes at lower MTR values of the MTR histogram and do not give a direct and accurate measurement of changes of pixel counts at the peak position of the MTR histogram.

Therefore, peak height, peak position, and mean MTR have a dimension of pixel counts and are sensitive to changes in the amplitude of the MTR histogram. In contrast, MTR_{25}, MTR_{50}, and MTR_{75} have a dimension of band size and are sensitive to changes in lower MTR values of the histogram. These parameters provide complementary information about the change in shape of the MTR histogram. Herein we sought to combine this complementary information by defining a new MTR histogram parameter, $AMTR_{2/3}$, which accounts for both the pixel count and the band size. Such a parameter is defined as the integration of the normalized two thirds of the peak height of the MTR histogram, $BSMTR_{2/3}$, as illustrated in Figure 1; the shaded area represents the area and integration from which $AMTR_{2/3}$ is calculated.

$AMTR_{2/3}$ is two dimensional in nature, because its value depends on both the peak height and the band of MTR values. However, unlike peak height, $AMTR_{2/3}$ does not count pixels at a single MTR value but rather pixels around the peak position. Unlike MTR_{25}, MTR_{50}, and MTR_{75}, the lower and upper limits of the MTR interval involved in $AMTR_{2/3}$ are not fixed but conditioned by the band size corresponding to two thirds of the peak height of the MTR histogram. Therefore, $AMTR_{2/3}$ simultaneously encodes information given by the parameters of peak height, peak position, and MTR values around the peak position. Owing to $BSMTR_{2/3}$, $AMTR_{2/3}$ also indirectly encodes information given by the MTR percentiles and is more sensitive to pixel count changes at lower MTR values than are peak height, peak position, and mean MTR.

The choice of band size corresponding to two-thirds the MTR histogram peak height in $AMTR_{2/3}$ is an important issue. In general, the MTR of any tissue varies among pixels. Therefore, counting pixels at a single MTR value, as in the case of peak height or peak position, or inside a small band of MTR values, as in the case of MTR_{25}, does not always allow one to characterize the MTR distribution of tissue in a pertinent way. At the other end of the continuum, if pixel counting is performed for the whole brain, as in the case of global MTR, or inside a large MTR band size beginning from zero, as in the case of MTR_{75}, the information is too averaged. This effect inevitably decreases the discriminating ability of the MTR parameters. With $AMTR_{2/3}$, an optimal MTR band size is involved. The decrease of the area under the histogram curve in two thirds of the peak height band size directly encodes the decrease of pixel counts around the MTR histogram peak and indirectly encodes the increase of pixels at lower MTR values.

Findings from the Present Study

The changes observed in the MTR histogram obtained in the patients with MS confirm what many researchers have found (4–6, 13, 14). However, different MTR parameters did not show the same discriminating ability. Among the previously reported parameters, peak height and MTR_{25} showed the largest relative difference and were therefore most sensitive to changes in the MTR histogram. This finding is consistent with theoretical definitions, as the two parameters capture changes in pixel counts at the peak location and in lower MTR values. Although peak height gave a bigger relative difference, it had a higher P value ($P = .07$) than that of MTR_{25} ($P = .004$) and was less discriminating than the latter (Figs 4 and 5). The same observation can apply to the comparison of P values for peak height versus other conventional parameters, such as global MTR ($P = .006$), mean MTR ($P = .006$), and MTR_{50} ($P = .06$). Peak height led to bigger SD and SD/mean values. This greater variability in peak height made it harder to differentiate patients from control subjects. These results demonstrate that peak height was sensitive to spurious variation, as expected.

The limitations of peak height, MTR_{25}, or other conventional parameters for discriminating control and injured groups has also been observed with other MT applications. McGowan et al (15) proposed the parameter, normal white matter range (RWM), which is defined as the mean of the white matter histogram ± SD. This parameter is sensitive to changes in the amplitude of the MTR histogram, but it is a better metric than peak height or other conventional MT parameters, because it involves integration over a band size of 2 SD. Compared with $AMTR_{2/3}$, RWM remains one dimensional in nature, because its band size is fixed (±SD). Greater variability of peak height compared with that of other conventional MT parameters can also be noted in early reports (8, 13, 14, 16–23). In many cases, this variability has contributed to higher P values for the peak height parameter. On the other hand, that MTR_{25} is more discriminating than are MTR_{50} and MTR_{75} directly demonstrates that MS can induce an important increase in pixel count at lower MTR values. The discriminating ability of MTR_{25}, MTR_{50}, and MTR_{75}

degraded when the histogram integration area increased. When 75% of the total histogram area was integrated, the discriminating ability was at its worst; this can be explained by an increase in the integration area that results in an overload of information. The large relative difference given by the peak height and MTR_{25} clearly suggests that MS causes simultaneous changes in pixel counts around the peak position and at lower MTR values of the histogram. Furthermore, a comparison of the relative difference of the peak height and MTR_{25} also shows that MS leads to more marked changes in pixel count at the peak location than in pixel count at lower MTR values. Among the parameters in Table 1, peak position and $BSMTR_{2/3}$ were the least discriminating. This finding implies that MTR band size alone is not sensitive to MTR histogram changes due to MS. (The peak position is a particular case in which the band size is reduced to one pixel.) In other words, the MS disease spectrum does not induce significant shifting of MTR histogram peak. Global MTR and mean MTR have an intermediate discriminating ability.

Compared with the previously reported parameters, $AMTR_{2/3}$ has shown the best discriminating ability. This finding demonstrates two important points. First, $AMTR_{2/3}$ preserves pixel-counting sensitivity of peak height but does not have the disadvantages of the latter with regard to spurious variations. Second, it also exhibits the ability of MTR_{25} for encoding changes at lower MTR values. In cases of MS, the band size of two-thirds peak height in $AMTR_{2/3}$ corresponds to a histogram area in which most of the pixels belonging to normal tissue are included, whereas pixels belonging to diseased tissue are excluded. If a larger band size is used, a larger area under the histogram curve would have been involved. As a result, pixels belonging to tissue affected by MS would be mixed with those corresponding to normal tissue. Likewise, if a smaller band size is used, pixels corresponding to normal tissue would not be taken into account. In both cases, the discriminating ability of the MTR parameters decreases. Therefore, the $BSMTR_{2/3}$ of $AMTR_{2/3}$ makes it possible to accurately capture changes in the MTR histogram due to MS by encoding simultaneous changes in pixel counts around the histogram peak position and at lower MTR values.

The difference in MTR histograms between the two control groups, as shown in Figure 3, shows that although the acquisition conditions were comparable in the two centers (ie, same MR imaging systems and protocol), the resulting MTR histograms differed in both shape and position. This difference might have been caused by several factors, such as difference in section thickness, but identifying the different causes is no trivial task. However, our results confirm findings showing that MTR measures are highly dependent on MR imaging units (21–26). In particular, Richert et al (25) have shown that for the same subject and the same MR imaging units, upgrading software can change the MTR histogram. These changes are characterized by both a modification in the peak height and a shift in the MTR histogram. Changes in the MTR histogram across MR imaging systems can be explained from an image-processing viewpoint. Calculating MTR accounts for a first-order derivation, with the difference in discrete images corresponding to the derivation of continuous images. It is well known that derivation is sensitive to spurious variations. If two images are not acquired under the same operating conditions, even small changes in images with and those without saturation pulses can be amplified on the resulting MTR image, leading to notable changes in the MTR histogram. In a multicenter study, it is generally difficult, if not impossible, to make the acquisition conditions exactly the same; no two MR imaging systems behave identically, even if they have the same hardware and software components.

The machine-dependent character of MTR measures poses the problem of how to distinguish between MTR changes due to disease and those due to system variations. The results in Table 2 illustrate this problem. The significant differences in conventional MTR values between the two control groups demonstrate that these parameters are not suitable for use in multicenter studies of MS. For example, peak height and MTR_{25} gave a particularly misleading indication by providing the greatest difference between the control groups. However, this failure of peak height, MTR_{25}, and other previously reported parameters is consistent with their one-dimensional nature. Existing parameters did not exhibit the same degree of failure. In particular, peak height gave a result better than that of other parameters. This indirectly implies that MTR histogram changes due to variation in MR imaging systems do not induce significant changes in pixel counts at the peak position of the histogram. That is, variation in MR imaging systems is not characterized by a decrease or increase in the number of pixels at the position of the histogram peak. This finding is somewhat consistent with that reported by Richert et al (25), which showed that the difference between the two MTR histograms in the same healthy control subject is characterized by clear MTR histogram shift on the MTR value axis. This MTR shifting can also be reflected in the large difference in the parameter peak position in Table 2.

Comparing the values of peak height in Tables 1 and 2 shows that the peak height is a better solution among the bad ones. We also note that the global MTR and mean MTR always exhibited intermediate performance. That the greatest difference was observed with MTR_{25} indicates that the modification of pixel counts at lower MTR values is an important characteristic of changes in the MTR histogram due to variations in MR imaging systems. Therefore, this variation induces not only shifting of MTR histograms but also substantial modifications in the MTR histograms at lower MTR values. As expected, these histogram modifications in the MTR histograms occurred with lower MTR values and these changes cannot be well described with existing MTR parameters. For example, histogram changes due to MS and

system variations are all characterized by increased pixel count at lower MTR, MTR_{25} and thus do not allow one to distinguish between patients with MS and healthy control subjects. In contrast, because the pixel counts at the peak position of the MTR histogram change significantly in patients with MS but little in control subjects, peak height is a more convenient parameter. Unfortunately, as explained earlier, peak height was sensitive to spurious variations; therefore, it did not provide the expected results of discrimination. The problem of stability with peak height can also be seen in its large SD/mean values (Table 2). On the contrary, the best performance was obtained with $AMTR_{2/3}$; this parameter was less affected by intersystem variability than were all other MTR parameters and maintained good ability in discriminating between patients and control subjects. This is not surprising; $AMTR_{2/3}$ integrates the histogram around a peak position and is therefore less sensitive to shifting of MTR histograms. Compared with peak height, which can be unsteady because it corresponds to pixel counts at a single MTR value, $AMTR_{2/3}$ is more stable because of correspondence to an integrated value within an interval of MTR values.

The design of the present investigation imitates that of a multicenter MR imaging trial in which subjects are imaged with different MR imaging systems at individual centers and in which a range of acquisition parameters is allowed for a given sequence. Therefore, we were not assessing pure intersystem variability, which is done by imaging the same group of control subjects with two MR imaging units and by using the same acquisition parameters. For this reason, interindividual and intersequence variations might have contributed to the observed differences in MTR parameters between the two control groups. However, because these variations correspond to practical situations in multicenter studies, our results reinforce the applicability of $AMTR_{2/3}$ as a potentially useful MTR parameter for the study of MS.

Conclusion

The previously proposed MTR parameters differ in terms of both sensitivity to MS-related abnormalities and susceptibility to intersystem variations in healthy control subjects. Although peak height and MTR_{25} are sensitive to changes due to MS, they do not allow one to distinguish these changes from those due to variations in MR imaging systems. The new MTR histogram parameter $AMTR_{2/3}$ seems to achieve the best trade-off between good discriminating ability and acceptable intersystem variability. This finding supports its use as a comprehensive, histogram-derived metric for the analysis of data in multicenter studies of MS monitored with MT MR imaging. Further clinical validation in larger subject databases and of clinical measures are the topics of our ongoing studies.

Acknowledgment

The authors would like to thank Mrs. M.P. Réthy, Medical Library, Hospital of Neurology of Lyon, for her technical assistance.

References

1. Filippi M, Grossman RI. **MRI techniques to monitor MS evolution: the present and the future.** *Neurology* 2002;58:1147–1153
2. van Waesberghe JH, Kamphorst W, De Groot CJ, et al. **Axonal loss in multiple sclerosis lesions: magnetic resonance imaging insights into substrates of disability.** *Ann Neurol* 1999;46:747–754
3. Dousset V, Grossman RI, Ramer KN, et al. **Experimental allergic encephalomyelitis and multiple sclerosis: lesion characterization with magnetization transfer imaging.** *Radiology* 1992;182:483–491
4. van Buchem MA, McGowan JC, Kolson DL, Polansky M, Grossman RI. **Quantitative volumetric magnetization transfer analysis in multiple sclerosis: estimation of macroscopic and microscopic disease burden.** *Magn Reson Med* 1996;36:632–636
5. Filippi M, Rocca MA, Minicucci L, et al. **Magnetization transfer imaging of patients with definite MS and negative conventional MRI.** *Neurology* 1999;52:845–848
6. Kalkers NF, Hintzen RQ, van Waesberghe JH, et al. **Magnetization transfer histogram parameters reflect all dimensions of MS pathology, including atrophy.** *J Neurol Sci* 2001;184:155–162
7. Filippi M, Inglese M, Rovaris M, et al. **Magnetization transfer imaging to monitor the evolution of MS: a 1-year follow-up study.** *Neurology* 2000;55:940–946
8. Sormani MP, Iannucci G, Rocca MA, et al. **Reproducibility of magnetization transfer ratio histogram-derived measures of the brain in healthy volunteers.** *AJNR Am J Neuroradiol* 2000;21:133–136
9. Lublin FD, Reingold SC. **Defining the clinical course of multiple sclerosis: results of an international survey—National Multiple Sclerosis Society (USA) Advisory Committee on Clinical Trials of New Agents in Multiple Sclerosis.** *Neurology* 1996;46:907–911
10. Kurtzke JF. **Rating neurologic impairment in multiple sclerosis: an expanded disability status scale (EDSS).** *Neurology* 1983;33:1444–1452
11. Miller DH, Barkhof F, Berry I, Kappos L, Scotti G, Thompson AJ. **Magnetic resonance imaging in monitoring the treatment of multiple sclerosis: concerted action guidelines.** *J Neurol Neurosurg Psychiatry* 1991;54:683–688
12. Wolff SD, Balaban RS. **Magnetization transfer contrast (MTC) and tissue water proton relaxation in vivo.** *Magn Reson Med* 1989;10:135–144
13. Patel UJ, Grossman RI, Phillips MD, et al. **Serial analysis of magnetization transfer histograms and Expanded Disability Status Scale scores in patients with relapsing-remitting multiple sclerosis.** *AJNR Am J Neuroradiol* 1999;20:1946–1950
14. van Buchem MA, Grossman RI, Armstrong C, et al. **Correlation of volumetric magnetization transfer imaging with clinical data in MS.** *Neurology* 1998;50:1609–1617
15. McGowan JC, Berman JI, Chetley Ford J, Lavi E, Hackney DB. **Characterization of experimental spinal cord injury with magnetization transfer ratio histograms.** *J Magn Reson* 2000;12:247–254
16. van Waesberghe JH, van Buchem MA, Filippi M, et al. **MR outcome parameters in multiple sclerosis: comparison of surface-based thresholding segmentation and magnetization transfer ratio histographic analysis in relation to disability—a preliminary note.** *AJNR Am J Neuroradiol* 1998;19:1857–1862
17. Filippi M, Iannucci G, Tortorella C, et al. **Comparison of MS clinical phenotypes using conventional and magnetization transfer MRI.** *Neurology* 1999;52:588–594
18. Iannucci G, Tortorella C, Rovaris M, Sormani MP, Comi G, Filippi M. **Prognostic value of MR and magnetization transfer imaging findings in patients with clinically isolated syndromes suggestive of multiple sclerosis at presentation.** *AJNR Am J Neuroradiol* 2000;21:1034–1038
19. Bozzali M, Rocca MA, Iannucci G, Pereira C, Comi G, Filippi M. **Magnetization-transfer histogram analysis of the cervical cord in patients with multiple sclerosis.** *AJNR Am J Neuroradiol* 1999;20:1803–1808
20. Rocca MA, Mastronardo G, Rodegher M, Comi G, Filippi M. **Long-term changes of magnetization transfer–derived measures**

from patients with relapsing-remitting and secondary progressive multiple sclerosis. *AJNR Am J Neuroradiol* 1999;20:821–827
21. Ostuni JL, Richert ND, Lewis BK, Frank JA. **Characterization of differences between multiple sclerosis and normal brain: a global magnetization transfer application.** *AJNR Am J Neuroradiol* 1999;20:501–507
22. Ge YL, Grossman RI, Udupa JK, Babb JS, Kolson DL, McGowan JC. **Magnetization transfer ratio histogram analysis of gray matter in relapsing-remitting multiple sclerosis.** *AJNR Am J Neuroradiol* 2001;22:470–475
23. Ge YL, Grossman RI, Babb JS, Rabin ML, Mannon LJ, Kolson DL. **Age-related total gray matter and white matter changes in normal adult brain, I: quantitative magnetization transfer ratio histogram analysis.** *AJNR Am J Neuroradiol* 2002;23:1334–1341
24. van Waesberghe JHTM, van Walderveen MAA, Castelijns JA, et al. **MR patterns of lesion development in multiple sclerosis: longitudinal observations using T1-weighted spin-echo and magnetization transfer MR.** *AJNR Am J Neuroradiol* 1998;19:675–683
25. Richert ND, Frank JA. **Magnetization transfer imaging to monitor clinical trials in multiple sclerosis.** *Neurology* 1999;53:S29–S39
26. Silver NC, Barker GJ, Miller DH. **Standardization of magnetic transfer imaging for multicenter studies.** *Neurology* 1999;53: S33–S39